

Ultra-High Energy Neutrinos: A Review of Theoretical and Phenomenological Issues

Raj Gandhi^a

^aHarish-Chandra Research Institute,
Jhusi, Allahabad, India 211019.

We review the phenomenology of UHE neutrino detection. The motivations for looking for such neutrinos, stemming from observational evidence and from the potential for new physics discoveries are enumerated, and their expected sources and fluxes are given. Cross-sections with nucleons at energies all the way upto 10^{20} eV and the attenuation of fluxes in the Earth, both of which are physics issues important to their detection, are discussed. Finally, sample event-rates for extant and planned Water/Ice Cerenkov detectors are provided.

1. Introduction

It is now widely believed that the recent Super Kamiokande (SK) result [1,2] of an anomaly in the flavour ratios and zenith angle dependence of the atmospheric neutrino flux provides the firmest signal yet of physics beyond the Standard Model (SM)¹. The significance of this can be gauged by the fact that a signal for such physics has been sought for in all the varied and intensive experimental probes that the many sectors of the SM have been subjected to over more than twenty-five years. That this signal comes from the neutrino sector of the theory perhaps assumes increased significance when considered in conjunction with the fact that two other existing experimental anomalies which persist, the solar deficit [4] and the LSND result [5] are also within the neutrino sector.

The detailed interpretation of these anomalies and their relation with each other is still a matter of intense and ongoing theoretical and experimental activity. However, neutrino masses, mixings and consequent oscillations have provided the simplest framework for understanding the experimental results [6]. What may be said with a reasonable degree of conviction is that once their interpretation is clear, a hitherto unprecedented window into the nature of the physical theory be-

yond the SM will probably have been opened.

It is within this context, perhaps, that one should view the theoretical and experimental efforts that are ongoing in the area of ultra high energy (UHE) neutrino physics (for reviews see [7-9]). If the physics excitement that we have uncovered in our study of low-energy neutrinos is an indicator, then the study of UHE neutrinos should pay rich dividends.

In view of the fact that data collection and further upgradation is ongoing for the first generation of UHE neutrino detectors (AMANDA [10] and BAIKAL [11]) and that planning, design, testing and deployment is underway for some others (AUGER [12], NESTOR [13], ICECUBE [14], ANTARES [15], RICE [16]), and NEMO [17]) definitive results of these efforts are still in the future. However, besides the other specific reasons from astrophysics and cosmic ray physics (some of which we discuss below) which provide motivation for such experiments, we note that the energy range covered by these experiments ($E_\nu \simeq 1$ TeV to 10^9 TeV or higher) offers an unprecedented opportunity for particle physics at energies significantly beyond the scope of terrestrial accelerators. Although progress is expected to be slow, the potential for serendipitous discovery is undoubtedly high.

In what follows, we give specific reasons why the search for UHE neutrinos can be expected to yeild positive results. Possible sources and their

¹The first hints of this anomaly were provided by atmospheric neutrino data from the IMB detector, [3]

fluxes are discussed. Salient features pertinent to the phenomenology of detection are then outlined, and sample rates provided.

2. Why should we search for and expect to detect UHE neutrinos?

In addition to the general particle physics motivations mentioned above, there exist specific reasons spanning several fields of research (astrophysics, astronomy, cosmic-ray physics and particle physics) for pursuing the search for UHE neutrinos. Motivation for their detection comes both from observational evidence hinting towards their production in astrophysical sites and the potential for new physics discoveries.

2.1. The Observed Cosmic-Ray Spectrum:

Perhaps one the strongest reasons comes from the observed cosmic-ray (CR) spectrum. We briefly discuss its observational features prior to making the connection to UHE neutrinos.

Over a period of several decades, a sizeable and impressive body of observations spanning twelve orders of magnitude in energy have been compiled by workers in this field. (For general discussions see [18,19], and for updates on observational efforts and data see [20].) An examination of the all-particle CR spectrum reveals a power-law behaviour over almost the entire spectral range, with breaks at what is referred to as the “knee” (corresponding to $E_{\text{primary}} \simeq 4 \times 10^{15}$ eV) and the “ankle” (corresponding to $E_{\text{primary}} \simeq 10^{19}$ eV).

Upto the knee region, the spectrum exhibits a power-law with index -2.7 , there onwards steepening to about -3 , and flattening again in the ankle region. The steep fall in the flux and the consequent increasing difficulty in detection is reflected in the fact that the number of primaries falls from about one particle per m^2 per sec at energies of about 10^{11} eV to roughly one per km^2 per century around the ankle (10^{19} eV).

It is thus necessary to employ very different techniques of detection depending on the energy of the primary. The direct observation of a CR primary is only possible in a detector mounted on a spacecraft or a balloon, due to interactions

in the atmosphere. Such detection, however can collect enough statistics only upto primary energies of about 10^{14} eV. At higher energies, indirect methods involving detection of secondaries produced by interaction of the primaries in the atmosphere is necessary. The most widely used indirect method has been the deployment of Extensive Air Shower (EAS) arrays (for example Yakutsk [21] and AGASA [22]). These sample a lateral cross-section of the multi-particle shower initiated by a CR primary high up in the atmosphere.

Clearly, the determination of the energy of the primary from the charged hadrons, electrons, muons and photons detected by the ground-based array is a non-trivial task. However, present Monte Carlo techniques allow this to be accomplished with an accuracy of about 30%. Still less trivial is the determination of the nature of the primary, which is complicated by fluctuations from shower to shower. In recent years another experimental technique, which focusses on the detection of secondary nitrogen fluorescence radiation excited by shower secondaries has been successfully implemented by Fly’s Eye [23].

Using the modes of detection discussed above, a general but incomplete picture of the nature of CR primaries has emerged. Essentially, below primary energies of 10^{14} eV, the composition is fairly accurately known, from a variety of direct detection experiments, to be 98% hadrons, mainly protons. Above these energies, where only indirect detection techniques can be employed, the composition appears to retain a significant hadronic fraction, even though the question as to whether the primaries are protons or heavier nuclei is yet unresolved. Very low statistics hampers any definitive conclusions about the composition of CR beyond the knee upto the highest energies (at and above the GKZ cutoff, which is discussed below). However, we stress that all or most of the by now numerous EAS events appear to have a muon content consistent with hadronic primaries.

For our purpose it is sufficient to say that it appears almost certain from the CR observations that there are astrophysical sites in the universe which accelerate hadrons upto energies of 10^{15} , and there is a reasonable probability that they

are accelerated to higher energies, perhaps all the way up to $\approx 10^{20}$ eV. The mechanisms by which this happens are not completely understood. Hadronic collisions, like $p + p$ or $p + \gamma$, always result in copious pion production. These follow the decay chain $\pi \rightarrow \mu + \nu_\mu, \mu \rightarrow e + \nu_\mu + \nu_e$ resulting in a flux ratio of 2:1 for $\nu_\mu : \nu_e$. The neutrino is expected to retain about 20% of the energy of the parent pion on the average, and in general, UHE neutrino fluxes are guaranteed if hadronic collisions play a role in UHE CR production. The precise shape of the spectrum, of course, depends on the nature of the source.

2.2. The GKZ Effect

In addition to neutrino production at the source, a UHE CR proton with energy in excess of about 5×10^{19} eV traversing interstellar space will interact with the Cosmic Microwave Background (CMB) to photo-produce pions, and hence neutrinos. (Representative fluxes are given in [24].) The interaction in question, the Δ resonance for single and multiple pion production, sets in at a center-of-mass energy of about 1.5 GeV and is responsible for an expected abrupt fall-off in the proton primary spectrum at and above these energies. This was first pointed out by Greisen, Kuzmin and Zatsepin [25,26] and is called the GKZ cutoff.²

2.3. Galactic CR Interactions with Interstellar matter

A diffuse UHE neutrino flux is also expected from interactions of galactic CR with interstellar matter, at energies around and below the knee region. For fluxes and related references, see [24]

2.4. Gamma-Ray Bursts

Yet another potentially important source of UHE neutrinos could be Gamma-Ray Bursts (GRB) [29]. There appears to be observational

² This cutoff is at present associated with one of the most significant puzzles in CR physics [27], because CR events with energies in excess of 10^{20} eV have been convincingly detected by several experiments employing different detection techniques [28]. We however, do not discuss this puzzle further in this article or the apparent absence of a GKZ cutoff signalled by the highest energy CR while emphasizing that the existence of the cutoff is demanded by well-tested low-energy SM physics.

support for a “fireball” model for GRBs [30]. The physics of this involves an initial merger or collapse of blackholes, neutron stars or some other highly magnetized compact object. The collapse to a small radius object is followed by a very rapid expansion, by about a factor of 10^5 in a time frame of the order of a second. This ultra-relativistic acceleration of the plasma of protons, electrons, positrons and photons leads, at some radius at which the plasma is optically thin to radiation which is detected as the GRB. At the same time, second-order Fermi shocks cause charged particle acceleration, and the ensuing $p - \gamma$ interactions lead to neutrino fluxes, which have been estimated in [31,32] for instance (See figure 1).

2.5. Active Galactic Nuclei

Active Galactic Nuclei (AGNs) are also expected to be an important source of UHE neutrinos. These are a class of highly compact bright objects powered presumably by black holes causing acceleration and accretion of matter, characterised usually by high powered jet emission. High energy gamma-rays (MeV, GeV and TeV) are expected and have been observed from ≈ 40 AGN sites. The acceleration of hadronic matter, as in proton-blazar models, again leads to subsequent $p - \gamma$ (and perhaps $p - p$) interactions, from which neutrinos are expected. (Figure 1). We note, however, that if only electrons are accelerated, as in the electron-blazar models, then a neutrino flux will be absent.

2.6. Topological Defects

There also exist mechanisms which do not involve the acceleration of matter but can still yield UHE fluxes of protons, photons and neutrinos. These are the “top-down” (TD) scenarios (for a comprehensive review of these see [33]) in which CR beyond the knee could originate in the decay of GUT scale massive particles produced due to topological defects like monopoles, cosmic strings, etc. Representative fluxes are shown in Figure 1.

2.7. Additional Physics Motivations

The detection of UHE neutrinos from all the above sources is expected to help answer many important questions in CR physics and the astro-

physics of highly energetic sources. Their detection above $10^{16} - 10^{18}$ eV from AGNs would provide important support for hadronic blazar (versus electron blazar) models.

Secondly, the observation of an isotropic neutrino flux beyond GKZ energies would signal that the events are due to universal CR activity rather than a nearby single source and would shed light on the nature of the primaries responsible for these events.

In addition, as emphasized in [31], very sensitive tests of gravitational couplings are possible via the detection of neutrinos co-related with GRB's.

Finally, important confirmation of the SK atmospheric result, which now firmly indicates that muon-neutrinos are most likely oscillating to tau-neutrinos, is possible. UHE Neutrinos which are produced by any of the modes or sources discussed above are not expected to have any significant component of ν_τ , originating as they do in $p - p$ and/or $p - \gamma$ interactions. However, the ultra-high energies and mega-parsec distances they travel prior to detection, when folded in with SK values for mass-squared differences and mixing angles, lead to a ν_τ component in the flux which is as large as the ν_μ and the ν_e components. The shadowing (in the earth) for ν_τ is interestingly different compared to that for ν_μ and ν_e , as pointed out in [34]. Specifically, the ν_τ component of the flux does not get significantly absorbed in the rock, but its energy spectrum gets modified, and its zenith angle distribution is relatively flat. The detection possibilities for such UHE ν_τ are discussed in [35,36].

3. UHE Neutrino Fluxes

In Figure 1 we show some of the flux calculations for UHE neutrinos from AGNs, GRBs and TD sources. We refer the reader to the references for details on the models used to obtain the predicted fluxes. The fluxes are labeled as AGN-M95 [37], AGN-SS91 [38], AGN-P96 [39] for Active Galactic Nuclei, GRB-WB [40] for Gamma Ray Bursts and TD-WMB12 [41], TD-WMB16 [41], TD-SLC [42] for top-down models. References and spectra for the remaining sources men-

tioned above may be found in [24], along with a discussion of their origins and sources.

It is important to stress here that fluxes for all the three sources in Figure 1 are still being modified as our understanding of the nature of the source, the interactions involved and the constraints placed by observations on them improve. For instance, it has been pointed out [56] that observations of the CR spectrum place important constraints on the neutrino flux from sources which are optically thin with respect to neutrons and photons. This argument could significantly restrict several AGN models, but the exact upper bound is presently being debated. In [57], for instance, it is argued that this bound depends on the assumption that the overall CR injection spectrum $dN/dE \propto E^{-2}$ upto energies of 10^{19} eV, and that injection spectra for many sources of CR producing shocks may be different, and, for a given source, may not extend all the way upto 10^{19} eV. The importance of using CR and other observations to constrain the physics occurring in the sources, and the neutrino fluxes emitted as emphasized in [56] however, cannot be disputed.

4. The Detection of UHE Neutrinos: General Considerations

Having discussed potential sources for UHE neutrinos, we next review some salient points relevant to their detection.

The main mode of detection discussed in the literature and implemented at extant detectors has been the observation of long range muons produced via charged current (CC) neutrino-nucleon interactions. The low fluxes necessitate the deployment of large volume water or ice detectors like AMANDA [10], BAIKAL [11], NESTOR [13] and ANTARES [15].

These are shielded from above by several kilometers of water-equivalent (kmwe) rock volume in order to suppress the otherwise overwhelming background from muons produced by CR interactions in the atmosphere. Indeed, for a considerable portion of the UHE range (100 TeV and lower), the detection of downward moving muons by Cerenkov radiation in water produced by contained events is less advantageous than that of

upward moving ones produced in the rock below the detector. The emphasis in existing detectors has thus been on looking mainly for muons which, after losses due to passage in the earth, still retain sufficient energy to be observed above threshold. In general, a 10 TeV muon will travel several km in rock before its energy is degraded down to 1 TeV, which is a typical detector threshold.³

Whereas serious neutrino astronomy results are not expected with present detector volumes, the actively underway upgradation of existing facilities and the addition of new ones should yield significant physics results in the next few years. The first AMANDA [10] detector has seen about 170 UHE atmospheric neutrino events, and its upgraded version, AMANDA II is presently taking data. A km³ extension, ICECUBE [14], is also planned. BAIKAL [11] has also observed UHE neutrinos and set limits on the UHE fluxes using its preliminary observation, with analysis of another 3 years of data currently underway. The ANTARES project [15], off the French coast, is exploring the design and implementation of a km³ scale deep sea detector for underground muons. Similarly, NESTOR [13] is doing the same southwest of the coast of Greece, while NEMO [17] is yet another planned deep sea detector off the southern Italian coast.

The RICE project in the Antarctic [16] will be a pioneering attempt to detect ν_e via radio waves. An UHE electron produced subsequent to a CC interaction in the rock transfers most of its energy to an electromagnetic shower. Positrons produced in the shower annihilate and additional atomic electrons scatter into the shower, causing a charge imbalance which corresponds to a ball of negative charge moving through the rock. The consequent Cerenkov emission gives radio waves

³A charged particle moving through rock suffers two types of energy losses, continuous and discrete. Continuous losses are mainly due to ionization of the medium, and their rate depends weakly (logarithmically) on the energy. Discrete losses stem from bremsstrahlung, electromagnetic interactions with nuclei and direct e^+e^- production. In general, such losses are proportional to the energy, but for muons gain importance only at higher energies. The most important loss mechanism, bremsstrahlung, is proportional to the inverse square of the mass of the charged particle, and hence is highly suppressed for muons relative to electrons.

($\lambda \simeq 10$ cm), which are detected by receivers buried in the ice.

Finally, the Pierre Auger Observatory [12], primarily designed to detect CR showers, should also be able to detect UHE neutrino induced showers close to the horizon. Rate calculations for this array are given in [9].

An important consideration for calculating event rates for muon neutrinos is the attenuation of neutrinos in the earth due to the rapid rise in the CC cross-section (discussed below) with energy. The interaction length of a neutrino in rock is approximately equal to the diameter of the earth at 40 TeV. A convenient quantity relevant to flux attenuation and event rate calculations is the 'shadow factor', S , which is defined to be an effective solid angle divided by 2π for upward muons and is a function of the energy-dependant cross-section for neutrinos in the earth [7]:

$$S(E_\nu) = \frac{1}{2\pi} \int_{-1}^0 d\cos\theta \int d\phi \exp[-z(\theta)/\mathcal{L}_{int}(E_\nu)]. \quad (1)$$

Here \mathcal{L} is the interaction length for the neutrino, defined by

$$\mathcal{L}_{int} = \frac{1}{\sigma_{\nu N}(E_\nu) N_A}, \quad (2)$$

where $N_A = 6.022 \times 10^{23} \text{ mol}^{-1} = 6.022 \times 10^{23} \text{ cm}^{-3}$ (water equivalent) is Avogadro's number. z represents the column-depth as a function of the nadir angle θ . Figure 3 (from Ref [7]) shows that from almost no attenuation at 10^{12} eV, about 93% of the flux is shadowed out at the highest energies at which CR have been observed ($\approx 10^{21}$ eV). It is this effect that makes the (low) downward rate for muons produced within the instrumented volume competitive with the upward rate at energies above 10^{15} eV, where the atmospheric background is essentially absent.

5. The Neutrino-Nucleon Deep Inelastic Scattering Cross-Section at UHE

Of crucial importance to the attenuation and the event-rate calculations is the UHE neutrino-nucleon DIS cross-section. This is given by

$$\nu_\mu N \rightarrow \mu^- + \text{anything}, \quad (3)$$

where $N \equiv \frac{n+p}{2}$ is an isoscalar nucleon, in the renormalization group-improved parton model. The differential cross section is written in terms of the Bjorken scaling variables $x = Q^2/2M\nu$ and $y = \nu/E_\nu$ as

$$\frac{d^2\sigma}{dxdy} = \frac{2G_F^2 ME_\nu}{\pi} \left(\frac{M_W^2}{Q^2 + M_W^2} \right)^2 [xq(x, Q^2) + x\bar{q}(x, Q^2)(1-y)^2], \quad (4)$$

where $-Q^2$ is the invariant momentum transfer between the incident neutrino and outgoing muon, $\nu = E_\nu - E_\mu$ is the energy loss in the lab (target) frame, M and M_W are the nucleon and intermediate-boson masses, and $G_F = 1.16632 \times 10^{-5}$ GeV $^{-2}$ is the Fermi constant. The quark distribution functions are

$$\begin{aligned} q(x, Q^2) &= \frac{u_v(x, Q^2) + d_v(x, Q^2)}{2} + \\ &\quad \frac{u_s(x, Q^2) + d_s(x, Q^2)}{2} + \\ &\quad s_s(x, Q^2) + b_s(x, Q^2) \quad (5) \\ \bar{q}(x, Q^2) &= \frac{u_s(x, Q^2) + d_s(x, Q^2)}{2} + \\ &\quad c_s(x, Q^2) + t_s(x, Q^2), \end{aligned}$$

where the subscripts v and s label valence and sea contributions, and u, d, c, s, t, b denote the distributions for various quark flavors in a proton. At the energies of interest here, perturbative QCD corrections are small and can safely be neglected. A parallel calculation similarly leads to the neutral-current cross section.

In our calculations we have used results from the ep collider HERA [43,?, 45–47] which have greatly enhanced our knowledge of parton distributions and are particularly significant for the present calculation. The usual procedure is to begin with parametrizations of parton distribution functions obtained from data at low values of Q^2 and evolve them to the desired high scale using the Altarelli-Parisi equations [49]. For UHE neutrino-nucleon scattering, however, the W -boson propagator forces increasing contributions from smaller and smaller values of x as the neutrino energy E_ν increases. In the UHE domain, the most important contributions to the

νN cross section come from $x \sim M_W^2/2ME_\nu$. Up to $E_\nu \approx 10^5$ GeV, the parton distributions are sampled at values of x where they have been constrained by experiment. At higher energies, we require parton distributions at such small values of x that direct experimental constraints are not available, not even at low values of Q^2 .

Thus the theoretical uncertainties that enter the evaluation of the UHE neutrino-nucleon cross section arise from the low- Q^2 parametrization, the evolution of the parton distribution functions to large values of $Q^2 \sim M_W^2$, and the extrapolation to small values of x . Of these, the last named contributes the greatest uncertainty.

In addition to the traditional approach, followed, for instance, in the CTEQ [48] distributions, (*i.e.*, to determine parton densities for $Q^2 > Q_0^2$ by solving the next-to-leading-order Altarelli-Parisi [49] evolution equations numerically) a second approach to small- x evolution attempts to solve the Balitskii-Fadin-Kuraev-Lipatov (BFKL) equation [50], which is a leading $\alpha_s \ln(1/x)$ resummation of soft gluon emissions. The BFKL approach predicts a singular behavior in x and a rapid Q^2 -variation,

$$xq_s(x, Q^2) \sim \sqrt{Q^2} x^{-0.5}. \quad (6)$$

On the other hand, applying the Altarelli-Parisi equations to singular input distributions $\propto x^{-\frac{1}{2}}$ leads to a less rapid growth with Q^2 ,

$$xq_s(x, Q^2) \sim \ln(Q^2) x^{-0.5}. \quad (7)$$

In the case of ultrahigh-energy neutrino-nucleon interactions, the region of interest is small- x and large- Q^2 , which requires a resummation of both $\ln 1/x$ and $\ln Q^2/Q_0^2$ contributions. An attempt to incorporate elements of the BFKL approach into the standard AP approach has recently been made in [51]. That this leads to cross-sections which are comparable (to within 10–15 % at the highest energies) with those obtained by next-to-leading order AP evolution is an indication that barring radically new physics, the cross-section calculation even at the highest energies is under control. Modifications in the cross-sections can occur, of course, as a result of physics beyond the SM. Many of these modifications are

strongly constrained by unitarity and for a broad class of plausible extensions are much smaller than the SM cross-section, as shown in [52]. Various other possibilities leading to higher neutrino-nucleon cross-sections have been discussed in the literature and some of the mechanisms considered include leptoquark excitations [53], superpartner contributions [54], strong FCNC interactions [55] and finally, higher dimensional gravitational contributions at TeV scales [61–64].

In Figure 2 (from [9]) we show the CC, NC and total cross-sections for $\nu - N$ interactions resulting from the SM using the AP approach to small x extrapolation.

6. Detection Rates

The event-rate for an underground detector of area A (events/sr/year) is calculable via

$$\text{Rate} = A \int_{E_\mu^{\min}}^{E_\nu^{\max}} dE_\nu P_\mu(E_\nu; E_\mu^{\min}) S(E_\nu) \frac{dN}{dE_\nu}. \quad (8)$$

Here $P_\mu(E_\nu, E_\mu^{\min})$ is the probability that a muon produced in a charged-current interaction arrives in a detector with an energy above the muon energy threshold E_μ^{\min} and is given by

$$P_\mu(E_\nu, E_\mu^{\min}) = N_A \sigma_{\text{CC}}(E_\nu) \langle R(E_\nu; E_\mu^{\min}) \rangle, \quad (9)$$

where $\langle R(E_\nu; E_\mu^{\min}) \rangle$ is the average range of a muon in rock. $S(E_\nu)$ is the shadow factor defined earlier and dN/dE_ν is the (isotropic) neutrino flux.

We give a set of sample rates below and refer the reader to [9] for a more extensive set of predictions..

Let us consider for illustration a detector with effective area $A = 0.1 \text{ km}^2$. This choice of size is intermediate to existing detectors and the planned future facilities. We show in Tables 1 and 2 the annual event rates for upward-going muons with observed energies exceeding 1 TeV and 10 TeV, respectively. We tabulate rates for the full upward-going solid angle of 2π , as well as for the detection of “nearly horizontal” muons with nadir angle θ between 60° and 90° . The predicted event rates, shown here for the CTEQ4-

DIS parton distributions, are very similar for other modern parton distributions.

We note that the atmospheric background overwhelms the signal when the threshold is 1 TeV. However, signals should emerge above background for 10 TeV and 100 TeV thresholds. Above 100 TeV, we have the rare case of “all signal and no background”, as the atmospheric muon flux disappears. Also evident in Table 2 is the effect of shadowing, with a majority of signal events in the “nearly horizontal” direction, where the neutrino traverses less rock prior to detection.

In addition to the (upward) partially contained events and the (downward) fully contained ones which become important at energies above which the atmospheric background disappears, it may be possible to detect cascade neutrino interactions at extremely high energies ($\geq 10^{17} \text{ eV}$) in the proposed Pierre Auger Cosmic Ray Observatory [12]. This will consist of both a ground array with detectors distributed over a very large area ($\approx 3000 \text{ km}^2$) and nitrogen fluorescence detectors. At these energies, the probability of a horizontally incoming neutrino interacting with the atmosphere is non-negligible. The events are thus rendered distinguishable from CR showers initiated by proton or other primaries by their incoming direction and their tendency to shower late into the atmosphere. The predictions for these are given in [9].

7. Conclusions

We have made an attempt to review the essential motivations and phenomenological issues related to the interactions and detection of UHE neutrinos and provided expected event rates for water/ice Cerenkov detectors.

Although present detector capabilities and sizes do not allow them to see above atmospheric backgrounds, with upgradations and several new large-scale experiments underway, the detection of UHE neutrinos from astrophysical sources may be very likely in the near future. Besides the potential for serendipitous discovery, the unmatched (terrestrially) energies may lead to new particle physics discoveries. In addition, these experiments may help clarify the astrophysical mech-

anism responsible for the ultra-relativistic acceleration of matter in these sources and answer important questions in CR physics, and, finally, provide sensitive tests of gravitational couplings and oscillations. For those working in UHE neutrino physics and astronomy, the anticipation is palpable.

8. Acknowledgements

I thank Chris Quigg, Mary Hall Reno and Ina Sarcevic for a stimulating collaboration, several results of which are presented here. I also acknowledge useful discussions over the years with Pijush Bhattacharjee, Gabor Domokos, Susan-Kovesi Domokos and Francis Halzen, who have contributed to my knowlwdge of UHE neutrinos.

Table 1

Upward $\mu^+ + \mu^-$ event rates per year arising from $\nu_\mu N$ and $\bar{\nu}_\mu N$ interactions in rock, for a detector with effective area $A = 0.1 \text{ km}^2$ and muon energy threshol d $E_\mu^{\min} = 1 \text{ TeV}$. The rates are shown integrated over all angles below the horizon and restricted to “nearly horizontal” nadir angles $60^\circ < \theta < 90^\circ$.

Flux	nadir angular acceptance	
	$0^\circ - 90^\circ$	$60^\circ - 90^\circ$
ATM [58]	1100.	570.
ATM [58] + charm [60]	1100.	570.
AGN-SS91 [38]	500.	380.
AGN-M95 ($p\gamma$) [37]	31.	18.
AGN-P96 ($p\gamma$) [39]	45.	39.
GRB-WB [31]	12.	8.1
TD-SLSC [59]	0.005	0.0046
TD-WMB12 [41]	0.50	0.39
TD-WMB16 [41]	0.00050	0.00039

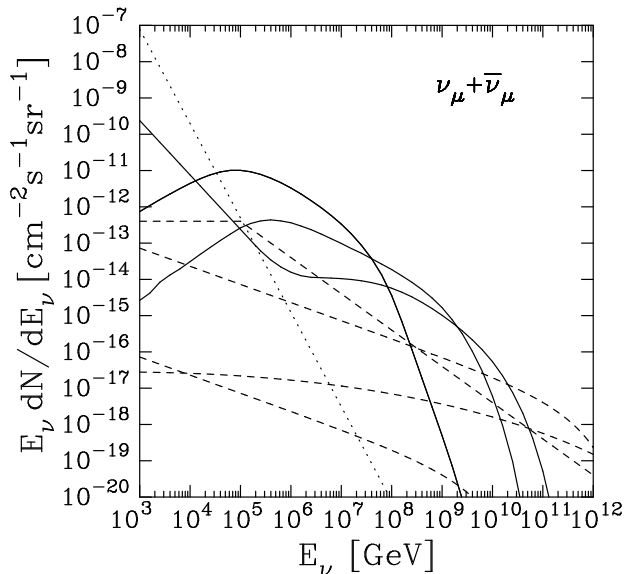


Figure 1. Muon neutrino plus antineutrino fluxes scaled by neutrino energy at the Earth’s surface. Solid lines represent AGN fluxes. In decreasing magnitude at $E_\nu = 10^3 \text{ GeV}$, they are AGN-M95, AGN-SS91 scaled by 0.3, and AGN-P96 ($p\gamma$). The dashed lines, in the same order, represent the GRB-WB, TD-WMB12, TD-WMB16, and TD-SLSC fluxes. The dotted line is the angle-averaged atmospheric (ATM) neutrino flux.

REFERENCES

1. Y. Fukuda *et. al*, Phys. Lett. **B 433**, 9 (1998); Phys. Rev. Lett. **81**, 1562 (1998).

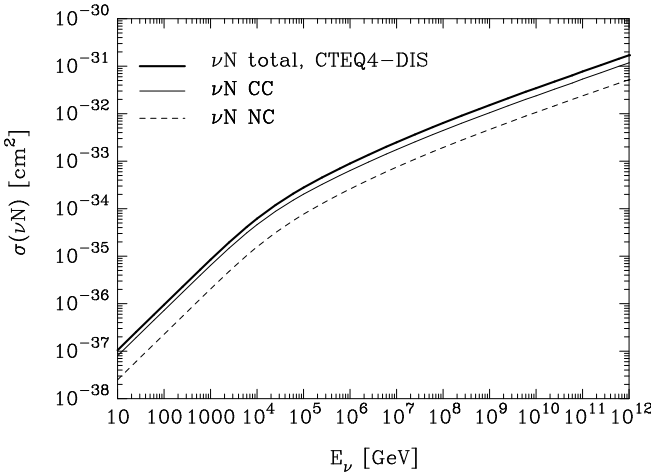


Figure 2. Cross sections for $\nu_\ell N$ interactions at high energies, according to the CTEQ4-DIS parton distributions: dashed line, $\sigma(\nu_\ell N \rightarrow \nu_\ell + \text{anything})$; thin line, $\sigma(\nu_\ell N \rightarrow \ell^- + \text{anything})$; thick line, total (charged-current plus neutral-current) cross section.

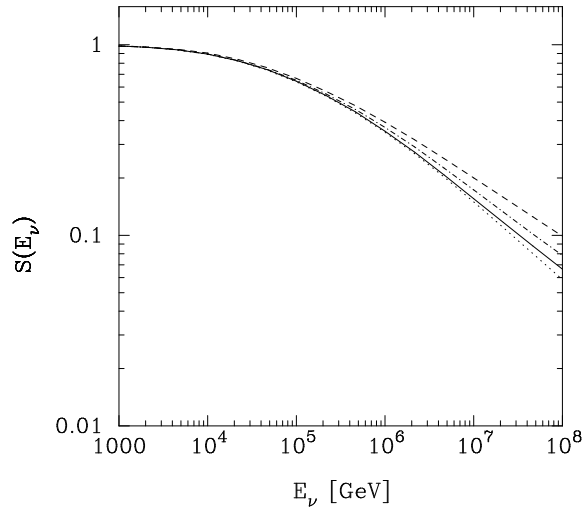


Figure 3. The shadow factor $S(E_\nu)$ for upward-going neutrinos assuming that $\sigma = \sigma_{\text{tot}}$ in (1) for CTEQ-DIS (solid line), CTEQ-DLA (dot-dashed) and D_- (dotted) parton distribution functions. Also shown is the shadow factor using the EHLQ cross sections (dashed line).

2. H. Sobel, talk at Neutrino 2000, these proceedings (see <http://nu2000.sno.laurentian.ca/>).
3. R. Becker-Szendy et al, Nucl. Phys. Proc. Suppl. **38**, 331, (1995).
4. For a discussion and references see, for instance, M. C. Gonzalez-Garcia and C. Pena-Garay, e-print hep-ph 0009041.
5. LSND Collaboration; C. Athanassopoulos et. al; Phys. Rev. Lett. **81**, 1774 (1998).
6. For a recent discussion, see, for instance, A. Smirnov, talk at Neutrino 2000, these proceedings (see <http://nu2000.sno.laurentian.ca/>).
7. R. Gandhi, C. Quigg, M. H. Reno and I. Sarcevic, Astroparticle Physics, **5**, 81, (1996);
8. T. Gaisser, F. Halzen and T. Stanev, Phys. Reports **258**, 173 (1995).
9. R. Gandhi, C. Quigg, M. H. Reno and I. Sarcevic, Phys. Rev. **D58** (1998) 093009.
10. E. Andres et al, (AMANDA Collaboration), e-print astro-ph 0009242 ; R. Wischnewski at al, *Nucl. Phys. B (Proc. Supp.)* **85** (19141) , , 2000.
11. For general information see <http://www.ihf.de/baikal/baikalhome.html>; also see V. Balkanov et al, (BAIKAL Collaboration), e-print astro-ph 0001151.
12. J. W. Cronin, Nucl. Phys. B (Proc. Suppl.) **28B** (1992) 213; The Pierre Auger Observatory Design Report (2nd edition), March 1997; see also <http://www.auger.org/>.
13. L. Resvanis, *Nucl. Phys. B (Proc. Supp.)* **87** (19448) , , 2000. Also see <http://www.uoa.gr/~nestor/>.
14. For general information see <http://www.ps.uci.edu/~icecube/workshop.html>; F. Halzen, Am. Astron. Soc. Meeting 192 (1998) # 62 28; AMANDA collaboration, e-print astro-ph/9906205, talk presented at the 8th Int. Workshop on Neutrino Telescopes, Venice, Feb 1999.
15. For general information see

Table 2

Upward $\mu^+ + \mu^-$ event rates per year arising from $\nu_\mu N$ and $\bar{\nu}_\mu N$ interactions in rock, for a detector with effective area $A = 0.1 \text{ km}^2$ and muon energy threshold $E_\mu^{\min} = 10 \text{ TeV}$. The rates are shown integrated over all angles below the horizon and restricted to “nearly horizontal” nadir angles $60^\circ < \theta < 90^\circ$.

Flux	nadir angular acceptance	
	$0^\circ - 90^\circ$	$60^\circ - 90^\circ$
ATM [58]	17.	10.
ATM [58] + charm [60]	19.	11.
AGN-SS91 [38]	270.	210.
AGN-M95 ($p\gamma$) [37]	5.7	4.3
AGN-P96 ($p\gamma$) [39]	28.	25.
GRB-WB [31]	5.4	4.0

<http://antares.in2p3.fr/antares/antares.html>; see also F. Montanet for the ANTARES Collaboration, *Nucl. Phys. B (Proc. Supp.)* **87** (1993) ,,, 2000, (e-print astro-ph 0001380); L. Thompson, these proceedings (<http://nu2000.sno.laurentian.ca/>).

16. For general information see <http://kuhep4.phsx.ukans.edu/~icema> n/index.html; also see C. Allen et al (RICE Collaboration), e-print astro-ph 9709223.
17. NEMO Collaboration, e-print hep-ex 0006031.
18. V. S. Berezinsky, S. V. Bulanov, V. A. Dogiel, V. L. Ginzburg, and V. S. Ptuskin, *Astrophysics of Cosmic Rays* (North-Holland, Amsterdam, 1990).
19. T. K. Gaisser, *Cosmic Rays and Particle Physics*, Cambridge University Press (Cambridge, England, 1990).
20. B. L. Dingus, *ed.* Proc. 26th *International Cosmic Ray Conference*, Utah, 1999, (AIP, New York, 2000).
21. N. N. Efimov et al., Proceedings of ICRR 90, Kofu, Japan, M. Nagano and F. Takahara, *eds.*, (World Scientific, Singapore, 1991), p. 20.
22. N. Hayashida et al., *Astrophys. J.* **522**, 225 (1999), e-print astro-ph 0008102; M. Takeda et al., *Phys. Rev. Lett.* **81** (1998) 1163; see also <http://icrsun.icrr.u-tokyo.ac.jp/as/project/agasa.html>.
23. D. J. Bird et al., *Phys. Rev. Lett.* **71** (1993) 3401; *Astrophys. J.* **424** (1994) 491; *ibid.* **441** (1995) 144.
24. R. Protheroe, Talk at Neutrino 98, astro-ph 9809144.
25. K. Greisen, *Phys. Rev. Lett.* **16** (1966) 748.
26. G. T. Zatsepin and V. A. Kuzmin, *Pis'ma Zh. Eksp. Teor. Fiz.* **4** (1966) 114 [*JETP. Lett.* **4** (1966) 78].
27. T. Weiler, these proceedings (or see <http://nu2000.sno.laurentian.ca/>).
28. A. Letessier-Selvon, these proceedings, (or see <http://nu2000.sno.laurentian.ca/>).
29. See E. Waxman, these proceedings, hep-ph 0009152
30. T. Piran, *Nucl. Phys. (Proc. Suppl.)* **70** (1999) 431; *Phys. Rept.* **314** (1999) 575.
31. E. Waxman and J. N. Bahcall, *Phys. Rev. Lett.* **78** (1997) 2292.
32. M. Vietri, *Phys. Rev. Lett.* **80** (1998) 3690.
33. P. Bhattacharjee and G. Sigl, preprint astro-ph 9811011, *Phys. Rep.* **327**, (2000), 109.
34. F. Halzen and D. Saltzberg, *Phys. Rev. Lett.* **81**, (1998), 4305 .
35. S. Iyer Dutta, M.H. Reno and I. Sarcevic, e-print hep-ph 0005310.
36. H. Athar, G. Parente and E. Zas, e-print hep-ph 0006123.
37. K. Mannheim, *Astropart. Phys.* **3** (1995) 295.
38. F. W. Stecker, C. Done, M. H. Salamon, and P. Sommers, *Phys. Rev. Lett.* **66**, 2697 (1991); *ibid.* **69** (1992) 2738E. Revised estimates of the neutrino flux appear in F. W. Stecker and M. H. Salamon, “High Energy Neutrinos from Quasars,” *Space Science Reviews* **75**, 341 (1996) (electronic archive: astro-ph/9501064), where it is assumed that all the observed AGN x-ray luminosity arises from hadronic interactions. We have scaled this flux by a factor of 0.3.
39. R. J. Protheroe, “High-Energy Neutrinos from Blazars” (electronic archive: astro-ph/9607165) in *Accretion Phenomena and*

Related Outflows, IAU Colloquium 163, Volume 121 of the ASP Conference Series, ed. D. T. Wickramasinghe, G. V. Bicknell, and L. Ferrario (Astronomical Society of the Pacific, San Francisco, 1997).

40. E. Waxman and J. Bahcall, Phys. Rev. Lett. **78**, 2292 (1997).
41. U. F. Wichoski, J. H. MacGibbon, and R. H. Brandenberger, “High Energy Neutrinos, Photons and Cosmic Rays from Non-Scaling Cosmic Strings,” BROWN–HET–1115 (electronic archive: hep-ph/9805419).
42. G. Sigl, S. Lee, D. N. Schramm and P. Coppi, Phys. Lett. **B392**, 129 (1997).
43. M. Derrick, *et al.* (ZEUS Collaboration), Phys. Lett. **B316** (1993) 412.
44. I. Abt, *et al.* (H1 Collaboration), Nucl. Phys. **B407** (1993) 515.
45. G. Wolf, “HERA Physics,” in *High Energy Phenomenology*, Proceedings of the 42nd Scottish Universities Summer School in Physics, St. Andrews, 1–21 August 1993, edited by K. J. Peach and L. L. J. Vick (SUSSP Publications, Edinburgh, and Institute of Physics Publishing, London, 1994), p. 135.
46. M. Derrick, *et al.* (ZEUS Collaboration), Z. Phys. **C65** (1995) 379.
47. T. Ahmed, *et al.* (H1 Collaboration), Nucl. Phys. **B439** (1995) 471.
48. H. Lai, *et al.* (CTEQ Collaboration), Phys. Rev. D **51** (1995) 4763.
49. G. Altarelli and G. Parisi, Nucl. Phys. **B126** (1977) 298. See also V. N. Gribov and L. N. Lipatov, Yad. Fiz. **15** (1972) 781 [English transl.: Sov. J. Nucl. Phys. **15** (1972) 438]; L. N. Lipatov, Yad. Fiz. **20** (1974) 181 [English transl.: Sov. J. Nucl. Phys. **20** (1974) 94]; Yu. L. Dokshitser, Zh. Eksp. Teor. Fiz. **73** (1977) 1216 [English translation: Sov. Phys.–JETP **46** (1977) 641].
50. E. A. Kuraev, L. N. Lipatov, and V. S. Fadin, Zh. Eksp. Teor. Fiz. **71** (1976) 840 [English translation: Sov. Phys.–JETP **44** (1976) 443]; Zh. Eksp. Teor. Fiz. **72** (1977) 377 [English translation: Sov. Phys.–JETP **45** (1977) 199]; Ya. Ya. Balitskiĭ, and L. N. Lipatov, Yad. Fiz. **28** (1978) 1597 [English transl.: Sov. J. Nucl. Phys. **28** (1978) 822]; L. N. Lipatov, Zh. Eksp. Teor. Fiz. **90** (1986) 1536 [English translation: Sov. Phys.–JETP **63** (1986) 904]; L. N. Lipatov, “Pomeron in Quantum Chromodynamics,” in *Perturbative Quantum Chromodynamics*, edited by A. H. Mueller (World Scientific, Singapore, 1989), p. 411.
51. J. Kwiecinski, A. Martin and A. Stasto, hep-ph 9905307.
52. G. Burdman, F. Halzen, and R. Gandhi, Phys. Lett. **B417**, 107 (1998).
53. M. A. Doncheski and R. W. Robinett, Phys. Rev. D. **56**, 7412 (1997); R. W. Robinett, Phys. Rev. D. **37**, 84 (1988).
54. M. Carena, D. Choudhury, S. Lola, and C. Quigg, Phys. Rev. **D58** (1998) 095003
55. J. Bordes, *et al.*, Astropart. Phys. **8** (1998) 135.
56. E. Waxman and J. Bahcall, Phys. Rev. **D59**, (1999) 023002.
57. J. Rachen *et al.*; astro-ph 9908031.
58. L. V. Volkova, Yad. Fiz. **31** (1980) 1510 [English transl.: Sov. J. Nucl. Phys. **31** (1980) 784].
59. G. Sigl, S. Lee, D. N. Schramm and P. Coppi, Phys. Lett. **B392**, 129 (1997).
60. L. Pasquali, M. H. Reno, and I. Sarcevic, “Lepton fluxes from atmospheric charm” (electronic archive: hep-ph/9806428).
61. N. Arkani-Hamed, S. Dimopoulos, and G. Dvali, Phys. Lett. B 429 (1998) 263; I. Antoniadis, N. Arkani-Hamed, S. Dimopoulos, and G. Dvali, Phys. Lett. B 436 (1998) 257; N. Arkani-Hamed, S. Dimopoulos, and G. Dvali, Phys. Rev. D 59 (1999) 086004.
62. G. Domokos and S. Kovács-Domokos, Phys. Rev. Lett. 82 (1999) 1366.
63. S. Nussinov and R. Shrock, Phys. Rev. D 59 (1999) 105002.
64. P. Jain, D. McKay, S. Panda, and J. Ralston, Phys. Lett B484, (2000) 267.